J. Phys. C: Solid State Phys., Vol. 7, 1974. Printed in Great Britain.

The electric quadrupole interaction in ZrO_2 and HfO_2

Y. Yeshurun and B Arad†
Department of Physics, Bar-Ilan University, Ramat-Gan, Israel

Received 16 July 1973

Abstract. The electric field gradients in ZrO_2 and HfO_2 have been measured by applying the differential perturbed angular correlation method to the 133–482 keV cascade in ^{181}Ta. The results for HfO_2 have been compared with previous results. In general, a fairly good agreement has been found except for the electric field asymmetry parameter η, in which the older result of Gerdau *et al*, rather than the more recent one of Gardner and Prestwich, has been confirmed. The results for ZrO_2 show the electric field gradient to be $(13{\cdot}3 \pm 0{\cdot}7) \times 10^{17}$ V cm^{-2} which is slightly higher than the value of $(12{\cdot}8 \pm 0{\cdot}6) \times 10^{17}$ V cm^{-2} obtained for HfO_2. The corresponding values for the field asymmetry are $0{\cdot}335 \pm 0{\cdot}015$ for ZrO_2 and $0{\cdot}348 \pm 0{\cdot}016$ for HfO_2. Despite the small difference of only 4% between the corresponding means, the 't' distribution shows, with confidence of better than 99%, that the results for ZrO_2 and HfO_2 are different.

1. Introduction

We have studied the static quadrupole interaction of ^{181}Ta nuclei with the electric field gradients existing in polycrystalline zirconia (zirconium dioxide) and hafnia (hafnium dioxide). The ^{181}Ta is a beta-decay product of ^{181}Hf and hence the latter nuclei must be present in all the substances to be analysed. These field gradients were measured by the differential perturbed angular correlation method (DPAC), which was applied to the 133–482 keV gamma cascade in ^{181}Ta. In these techniques one measures the angular distribution of one gamma ray with respect to the other, as a function of time. The ordinary angular distribution function is modified by a time-dependent factor ($G_{22}(t)$ in equation 1). This factor is caused by the interaction of the internal electric field gradients with the nuclear quadrupole moment during the lifetime of the excited level. Studies of the electric field gradients in hafnia have been carried out by several groups (Salomon *et al* 1964, Marest *et al* 1966, Gerdau *et al* 1969 and Gardner and Prestwich 1970) while no such measurement has been reported for zirconia. We decided to repeat the measurements in hafnia for two reasons: (i) To compare the consistency of our results with those published in the literature and to be able to compare the results of zirconia with those of hafnia; (ii) To measure the asymmetry parameter η which Gardner and Prestwich found to be smaller than the value given by Gerdau *et al* by as much as three standard deviations.

Hafnium is a natural contaminant in all the zirconium minerals because their chemistry is almost identical. Of all the elements, zirconium and hafnium are the two most difficult to separate. In addition, both elements have almost the same atomic radius

† Also: Department of Nuclear Physics, Soreq Nuclear Research Centre, Yavne, Israel.

(1·55 Å). Furthermore, hafnia and zirconia have almost the same interatomic distances (2·2 Å) and the same space group (Slater 1965). The phase diagram for the solid solution $(HfO_2)_x$ $(ZrO_2)_{1-x}$ shows the same monoclinic crystal structure for all the values of $x(0 \leqslant x \leqslant 1)$ and there are no phase transitions for temperatures below 1100 K. For all these reasons we believe that the HfO_2 molecules are homogeneously distributed among the ZrO_2 molecules and hence the ^{181}Ta nucleus—which is formed in the ^{181}Hf decay—occupies a regular crystal site.

2. Experimental

About 2 mg of HfO_2 were irradiated for a day in the 5MW nuclear reactor at the Soreq Nuclear Research Centre. The ZrO_2 included about 1·3% of HfO_2, and so some 20 mg of ZrO_2 were irradiated for a period of 4 days. Both samples were annealed for two days at 1100 K. Higher temperatures were not attempted in order not to cross the transition boundary into the tetragonal phase (see figure 1).

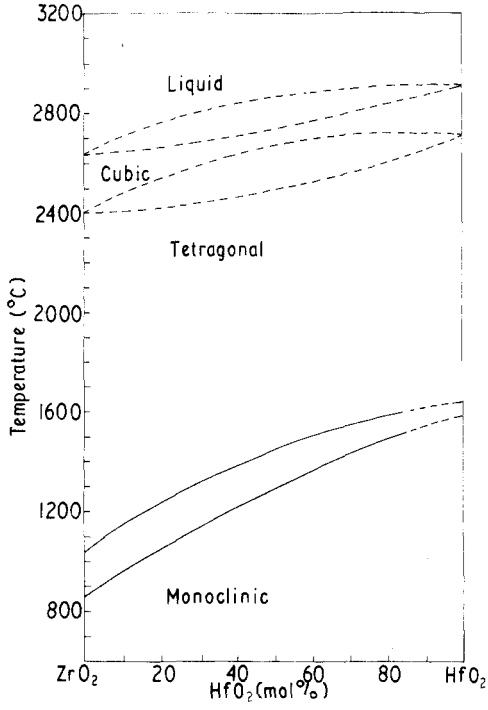

Figure 1. The phase diagram of the solid solution ZrO_2–HfO_2. The upper lines were obtained in the heating procedure while the lower ones were obtained in cooling procedure (from Ruh *et al* 1968).

In order to check our assumption regarding the distribution of hafnia in zirconia, the zirconia powder was analysed with an electron microprobe. The results have confirmed our assumptions, ie that the hafnium dioxide molecules are homogeneousely distributed among the zirconium dioxide molecules.

The electronic system used is the usual fast–slow arrangement (figure 2). The 133 keV gamma rays were detected in $1\frac{1}{2}$ in diameter $\frac{1}{4}$ in thick NaI crystal coupled to an RCA 8575 photomultiplier. The fast anode pulse was amplified and fed into two fast discriminators. After proper delay adjustments both output pulses were overlapped in the EG & G coincidence unit (figure 3). When one discriminator was adjusted to the

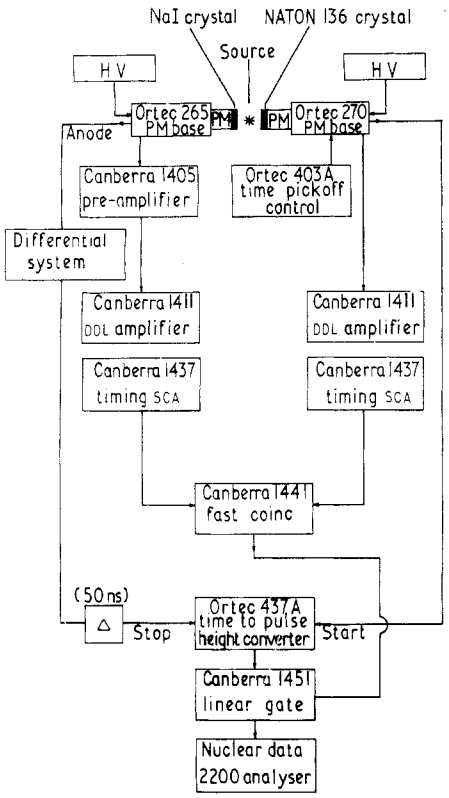

Figure 2. The electronic system.

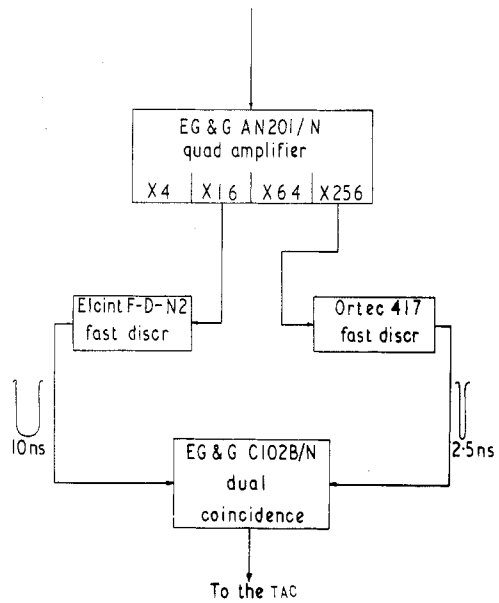

Figure 3. The differential arrangement.

first photoelectron level and the other discriminator to the level of a few keV, a time resolution of 1·1 ns FWHM was obtained without increasing the random coincidences due to unwanted noise counts. The 482 keV gamma rays were detected in a $1\frac{1}{2}$ in diameter 1 in thick Naton 136 plastic scintillator coupled to an RCA 8575 photomultiplier. The fast pulses were processed in a constant-fraction discriminator. The energy restriction in the slow channel was adjusted to the upper 10–20% of the 482 keV Compton edge.

Time curves of the 15·6 ns mean life 482 keV level in ^{181}Ta were taken with both detectors subtending angles of 90°, 180°, 270° and 180° for periods of 24 hours at each angle. The results obtained at angles of 90° and 270° were added and combined with those obtained at 180°. With such a procedure, any effects which may result from a slight incorrect centering of the sample will cancel out to the first order. The time scale of the multichannel analyser was measured by feeding the time to amplitude converter (TAC) from a Tennelec 850 calibrator unit.

3. Data analysis and results

The angular distribution function $W(\theta, t)$ is given in equation (1) (see for example Frauenfelder and Steffen, 1965)

$$W(\theta, t) = 1 + A_{22}G_{22}(t)P_2(\cos\theta), \tag{1}$$

where higher-order terms have been neglected. In order to extract $G_{22}(t)$, measurements at $\theta = 180°$ and $\theta = 90°$ or 270° were carried out. Inserting the experimental values into equation (1) and solving for $G_{22}(t)$ one obtains

$$G_{22}(t) = \frac{2}{A_{22}} \frac{W(180, t) - W(90, t)}{W(180, t) + 2W(90, t)}. \tag{2}$$

The perturbation function can be written (Beraud *et al* 1969, Gerdau *et al* 1969)

$$G_{22}(t) = \sum_{n=0}^{3} \sigma_{2n} \cos(\omega_n t) \tag{3}$$

When the finite time resolution for the electronic system and the deviations in the hyperfine fields due to crystal inperfections are taken into account, equation (3) is modified. One finds that

$$G_{22}(t) = \sum \sigma_{2n} \exp(-\tfrac{1}{2}\omega_n^2 \tau^2) \exp(-\tfrac{1}{2}\omega_n^2 \delta^2 t^2) \cos(\omega_n t), \tag{4}$$

where $2\sqrt{2}\ln 2\tau$ is the FWHM of the time response function of the system and δ has a similar meaning for the frequency distribution around the average frequency.

The electric field gradients in a crystal are characterized by the greatest component V_{zz} and the asymmetry parameter η defined by

$$\eta = \frac{V_{xx} - V_{yy}}{V_{zz}} \tag{5}$$

where $|V_{zz}| > |V_{yy}| > |V_{xx}|$.

The interaction hamiltonian for $I = \frac{5}{2}$ when diagonalized (Beraud *et al* 1969) yields a cubic equation for the eigenvalues of the nuclear quadrupole hamiltonian (in units of $\hbar\omega_Q$) as a function of the asymmetry parameter η. The differences between the energies, divided by $\hbar$, are transition frequencies ω_n appearing in equation (3). On obtaining the frequencies ω_n the parameter η can be deduced from the ratio ω_2/ω_1.

The quadrupole interaction frequency is given by

$$\omega_Q = eQV_{zz}/4\hbar I(2I - 1). \tag{6}$$

When ω_1 and η are known, these values can be inserted in the cubic equation and the quadrupole frequency ω_Q deduced. On inserting the values for the 482 keV level in ^{181}Ta, $I = \frac{5}{2}$, $Q = 2{\cdot}53 \pm 0{\cdot}10$ barn†, (Gardner and Prestwich 1970) the field gradient V_{zz} is obtained.

In order to obtain the three frequencies ω_i, $i = 1, 2, 3$, the power spectrum of equation (2) was calculated using the IBM subroutine 'FORIT'. In order to improve the frequency resolution of the power spectrum, the time interval was enlarged (Forker and Rogers 1971). The power spectra of the same experiment with two different time intervals can be seen in figures 4 and 5.

† Actually, in accordance with a more recent value of Q_0 (Löbner *et al* 1970) Q should have been taken as 2·41 barn. However, in order to be able to compare our results with previous ones, the value of 2·53 barn was used.

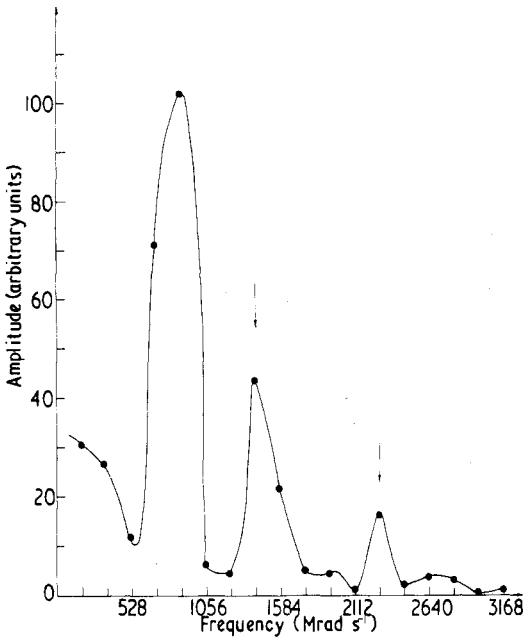

Figure 4. A typical power spectrum of HfO_2. $T = 35$ ns; $\Delta\omega \simeq 176$ Mrad s^{-1}.

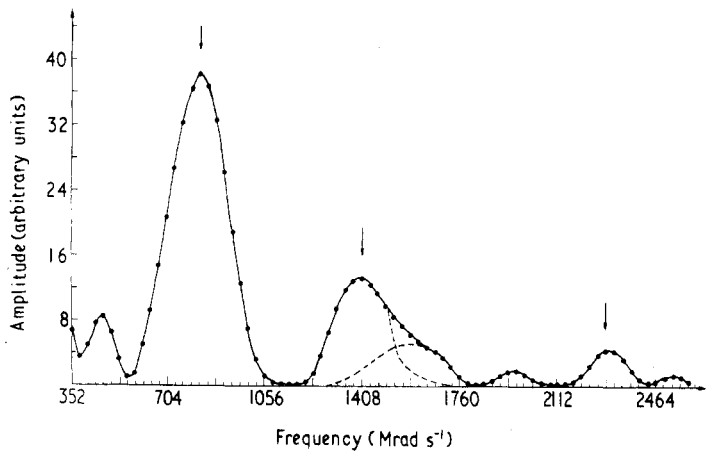

Figure 5. The power spectrum of the same results as figure 4 after the time scale was enlarged sixfold by adding zeros to the time base. The three main frequencies are indicated by arrows. $T_0 \simeq 35$ ns; $T = 6T_0$; $\Delta\omega = 29{\cdot}34$ Mrad s^{-1}.

As an alternative approach, nonlinear least-square fitting was used to deduce the six parameters ω_1, ω_2, ω_3, A_{22}, δ and t_0 where t_0 is a time factor to adjust the correct phase. All the other parameters are as defined previously. Although ω_3 is not an independent parameter, it was used as such in order to check the consistency of the results, ie that $\omega_1 + \omega_2 = \omega_3$. Figure 6 shows a typical nonlinear least-squares fit of equation (4) (multiplied by the experimental factor A_{22}) to the experimental results.

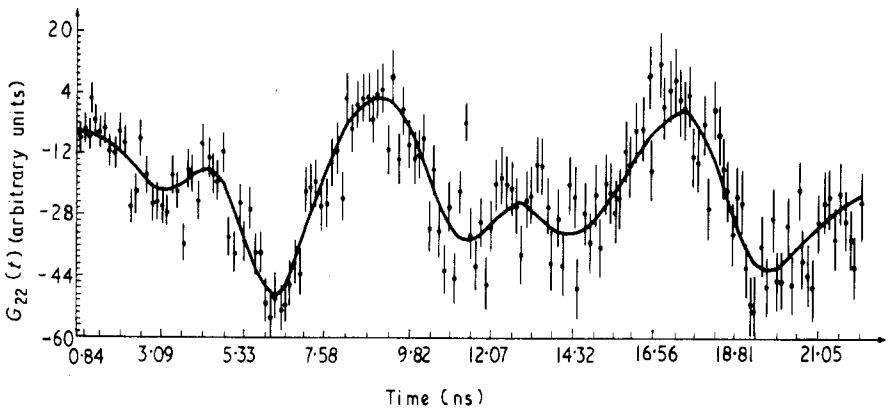

Figure 6. A typical nonlinear least-square fit of the experimental results as given in equation (2) to the theoretical expression as given in equation (4). The vertical scale is actually $\frac{1}{2}A_{22}^{\exp} \times G_{22}(t)$.

Tables 1 and 2 show the values obtained for ω_1, ω_2, ω_3 and ω_2/ω_1 for HfO_2 and ZrO_2. All the runs in a subgroup were obtained under the same conditions, while the different subgroups were obtained under different irradiation conditions and/or different geometrical conditions.

Table 1. The three frequencies and the frequency ratio for HfO_2 as obtained by least-squares fitting

ω_1	ω_2 (Mrad s^{-1})	ω_3	ω_2/ω_1	Remarks
823	1446	2256	1·757	A
832	1420	2210	1·707	
839	1469	2354	1·751	
810	1423	2207	1·757	B_1
825	1436	2223	1·741	
837	1461	2306	1·746	
857	1448	2226	1·690	
844	1467	2388	1·738	B_2
837	1477	2364	1·765	
835	1462	2346	1·751	
826	1436	2297	1·738	
832	1444	2291	1·736	
819	1429	2190	1·745	B_3
820	1446	2221	1·763	
802	1377	2212	1·717	B_4
840	1445	2244	1·720	
830 ± 14	1443 ± 24	2271 ± 65	1·739 ± 0·020	Averaged

A and B are different samples obtained under different irradiation conditions. B_i are the same sample measured under different geometrical conditions. The statistical inaccuracy of the individual frequencies is 2%–3%.

Table 2. The three frequencies and the frequency ratio for ZrO_2 as obtained by least-squares fitting

ω_1	ω_2 (Mrad s^{-1})	ω_3	ω_2/ω_1
868	1527	2320	1·759
810	1406	2258	1·736
833	1451	2229	1·742
877	1522	2434	1·735
858	1541	2447	1·796
889	1571	2522	1·767
847	1479	2312	1·746
837	1499	2213	1·791
848	1470	2234	1·733
893	1560	2426	1·747
882	1512	2236	1·714
889	1575	2435	1·772
811	1458	2209	1·798
859	1525	2367	1·775
881	1544	2414	1·753
879	1551	2471	1·765
899	1570	2407	1·746
847	1465	2302	1·730
839	1477	2339	1·760
852	1495	2311	1·755
821	1439	2212	1·753
817	1427	2195	1·747
823	1448	2200	1·759
837	1456	2242	1·740
838	1462	2269	1·745
853 ± 27	1497 ± 49	2320 ± 99	1·755 ± 0·020

The various subgroups describe different samples and irradiation conditions. The statistical inaccuracy of each individual frequency is 2%–3%

Table 3. The results for ZrO_2 and HfO_2

Sample	No. of runs	ω_1	ω_2 (Mrad s^{-1})	ω_3	η	ω_Q (Mrad s^{-1})	V_{zz} 10^{17} V cm^{-2}	Remarks
HfO_2	16	830 ± 14	1443 ± 24	2271 ± 65	0·348 ± 0·016	123·1 ± 2·4	12·8 ± 0·6	LQ
HfO_2	14	834 ± 34	1463 ± 48		0·332 ± 0·059	124·8 ± 3·6	13·0 ± 0·7	FT
ZrO_2	25	853 ± 27	1497 ± 49	2320 ± 99	0·335 ± 0·015	127·5 ± 4·2	13·3 ± 0·7	LQ
ZrO_2	20	849 ± 25	1506 ± 55		0·321 ± 0·045	127·9 ± 4·9	13·3 ± 0·8	FT

LQ: Least squares; FT: Fourier transform.

The results deduced for HfO_2 and ZrO_2 are summarized in table 3. Using the '*t*' test of significance between two sample means (see for example Fisher 1958)

$$t = (\bar{X}_1 - \bar{X}_2)\left[\left\{\left(\sum_{i=1}^{N_1}(X_{1i} - \bar{X})^2 + \sum_{i=1}^{N_2}(X_{2i} - \bar{X}_2)^2\right)\Big/(N_1 + N_2 - 2)\right\} \times \left(\frac{1}{N_1} + \frac{1}{N_2}\right)\right]^{-1/2} \quad (7)$$

one obtains for ω_1 the value of $t = 3{\cdot}18$ with 39 degrees of freedom and for ω_2/ω_1 (and hence also for η) the value of $t = 2{\cdot}40$ with 39 degrees of freedom. From such large values one can conclude that the probability of HfO_2 and ZrO_2 having the same frequency ω_1 is less than 1% and that of their having the same electric field asymmetry parameter η is less than 3%.

4. Discussion

In table 4 we compare the present results for HfO_2 with results obtained previously by

Table 4. The results for HfO_2 as obtained by various research teams

	Present results		Gardner and Prestwitch	Gerdau *et al*	
	LQ	FT	FT	FT	LQ
ω_1 (Mrad s^{-1})	830 ± 14	834 ± 34	819 ± 10	843 ± 8	—
ω_2 (Mrad s^{-1})	1443 ± 24	1463 ± 48	1483 ± 25	1435 ± 10	—
ω_3 (Mrad s^{-1})	2271 ± 65	—	2350 ± 50	2323 ± 56	—
ω_Q (Mrad s^{-1})	123·1 ± 2·4	124·8 ± 3·6	125·8 ± 1·9	122·4 ± 2·5	126·9 ± 1·3
η	0·348 ± 0·016	0·332 ± 0·049	0·283 ± 0·027	0·38 ± 0·03	0·35 ± 0·03
V_{zz} ($\times 10^{17}$ V cm^{-2})	12·8 ± 0·7	13·0 ± 0·6	13·1 ± 0·6	—	13·2 ± 0·6

LQ: Least squares; FT: Fourier transform

Gerdau *et al* (1969) and Gardner and Prestwich (1970). No meaningful results could be obtained with an unannealed sample. The present results were all obtained after two days of annealing and hence only the similar results of Gerdau *et al* are mentioned despite the fact that they had an additional annealing period of 4 hours at 1500 K. It can be seen that the present result for ω_1 are in excellent agreement with both the results of Gerdau *et al* and of Gardner and Prestwich while the result for η agrees with those of Gerdau *et al* but disagrees with the lower value of Gardner and Prestwich. These latter authors explained their lower value as compared with the value of Gerdau *et al* by their having a better time resolution (1·3 ns and 2·4 ns respectively). The time resolution of the present experiment (1·1 ns) which confirms the result of Gerdau *et al*, shows that the low value is not due to the improved time resolution but probably due to an undiscovered non-statistical bias.

Gerdau *et al* also deduced the frequency distribution δ. We find in our results that δ and A_{22} are strongly linked together. A change of ±10% in A_{22} which causes a change of ± 70% in δ (leaving all the other parameters practically unaltered) changes χ^2 by not more than ±5%. Unfortunately, most of our measurements were carried out under different geometrical conditions for which we did not have independent information on A_{22}, and hence, we were not able to deduce meaningful information about δ.

On comparing the results for the field gradient V_{zz} and the asymmetry parameter η for ZrO_2 and HfO_2 one finds that each result for one oxide is displace from the other result by about one standard deviation only. However as these results are sample averages of several runs the 't' distribution shows with confidence of better than 99% that the means belong definitely to different populations and hence the 4% differences in V_{zz} and η are real.

Calculations are required (and are being undertaken in this laboratory) to see to what extent these differences can be explained by the small differences in the crystal structure. If this is not so, the changes will have to be attributed to the effect of the next-nearest neighbours (the nearest neighbours are oxygen atoms common to both salts) in which the outer $4d^25s^2$ electrons of Zr are replaced by the $5d^26s^2$ electrons in Hf.

References

Beraud R, Berkes I, Daniere J, Marest G and Rougny R 1969 *Nucl. Instrum. Meth.* **69** 41
Fisher R A 1958 *Statistical Methods for Research Workers* 13th ed (Edinburgh: Oliver and Boyd) p 122
Forker M and Rogers J D 1971 *Nucl. Instrum. Meth.* **96** 453
Frauenfelder H and Steffen R M 1965 in *Alpha, Beta and Gamma Ray Spectroscopy* ed Siegbahn (Amsterdam: North Holland) pp 997–1198
Gardner P R and Prestwich W V 1970 *Can. J. Phys.* **48** 1430
Gerdau E, Wolf J, Winkler H and Braunfurth J 1969 *Proc. R. Soc.* A **311** 197
Löbner K E G, Vetter M and Hönig V 1970 *Nucl. Data Tables* **A7** 495–564
Marest G, Berkes I, Bougnot G and Beraud I 1966 *C.R. Acad. Sci., Paris* B **262** 367
Ruh R, Garret H J, Domagal R F and Tallan N M 1968 *J. Am. Ceramic Soc.* **51** 23
Salomon M, Bostrom L, Lindqvist T, Perez M and Zwanziger M 1964 *Ark. Fys.* **27** 97
Slater J C 1965 *Quantum Theory of Molecules and Solids* vol 2 (New York: McGraw-Hill)